

Adsorption of Methylene Blue from Aqueous Solution Using Locust Bean Gum graft Copolymer-Bentonite Composite

Sirajo Abubakar Zauro^{1,2*}, Vishalakshi Badalamoole¹
and Haruna Shehu Ahmed³

¹*Department of Post-Graduate Studies and Research in Chemistry, Mangalore University, Mangalagangothri, Karnataka, India.*

²*Department of Pure and Applied Chemistry Usmanu Danfodiyo University, Sokoto, Nigeria.*

³*Nigerian Defence Academy, Kaduna.*

Original Research Article

ABSTRACT

A graft copolymer gel composite made up of locust bean gum (LBG), diallyldimethylammonium chloride (DADMAC), 2-acrylamido-2-methyl-1-propane sulfonic acid (AMPS) and bentonite (BNT) was prepared using methylenebisacrylamide (MBA) as crosslinker via microwave irradiation and characterised using FTIR, FESEM/EDS and XRD techniques. The grafted copolymer composite was evaluated for its adsorption towards methylene blue (MB) dye. The LBG-g-poly(DADMAC-co-AMPS)/BNT showed a maximum adsorption of 70.89 mg/g compared to 65.09 mg/g showed by LBG-g-poly(DADMAC-co-AMPS). The adsorption data were subjected to two different isotherm

*Corresponding author: E-mail: sirajozauro@gmail.com;

models namely; Freundlich and Langmuir and were observed to be explained best by the Freundlich model. The adsorption of MB on the graft copolymer gel and the composite is observed to be a second-order kinetic process.

Keywords: Adsorption; bentonite; diallyldimethylammonium chloride; methylene blue; locust bean gum; 2-acrylamido-2-methyl-1-propane sulfonic acid.

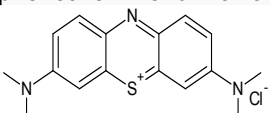
1. INTRODUCTION

The use of synthetic materials such as dyes for various industrial uses (textile, leather, paper, rubber, plastic, cosmetic etc.) has lead to the proportionate discharge of a large quantity of effluent containing non-biodegradable, toxic and carcinogenic coloured substances into the environment. This becomes increasingly a major threat to water bodies and the removal of those pollutants from wastewater by means of an environmentally friendly technique is a major challenge [1-4].

Methylene blue (MB) is a cationic dye utilise in various fields such as Biology, Chemistry, medical sciences and textile industries. The long-term exposure to MB can cause nausea, vomiting and anaemia [5].

Some of the physicochemical properties of MB are shown in Table 1.

Table 1. Physical properties of methylene blue dye

IUPAC name	3,7-bis(Dimethylamino)-phenothiazin-5-ium chloride
Structure	
Molecular formula	C ₁₆ H ₁₈ ClN ₃ S
Molar mass	319.85 g/mol
colour	dark green crystalline powder
Solubility	Soluble in water and ethanol
λ_{max}	663nm

Several techniques such as chemical precipitation, ion exchange, membrane separation, chemical reduction, chemical oxidation, advanced oxidation processes [6] have been employed in the removal of toxic substances from the environment. The efficiency of the above techniques to remove the dye molecules are still low and the methods are time-consuming, expensive and sometimes generate a large amount of sludge which is toxic to the

living organisms in the environment. Hence, adsorption using composite based biopolymers has been described as one of the most effective and promising technique for removal of such pollutants [7-9].

Locust bean gum (LBG) is a polysaccharide of high molecular weight that is extracted from the seed of carob tree *Ceratonia siliqua* [10]. LBG consist of a β -1-4-D-mannose chain substituted at the 6 positions on varying degree with single α -linked D-galactose residues [11]. It consists mainly of galactose and mannose in 1:4 ratio and is largely known as glactomannose. It has a range of molecular weight between 3×10^5 to 1.2×10^6 DA. It is non ionic, hence its properties unaffected by pH changes within the range of 3-11 or ionic strength [12]. LBG has a wide range of applications in fields such as drug delivery [13], water sorption [14], emulsification and gelation [15] etc.

The polymer-clay composite has been gaining increased attention by researchers globally due to the hybrid properties they exhibit when compared with either the polymer or clay separately. A wide range of polymer-clay composite has been produced and used for water treatment [16,17], dye adsorption [18,19] etc.

The synthesis of ionic copolymers has been gaining significant interest among researchers [20]. Diallyldimethylammonium chloride (DADMAC) is one of the water-soluble cationic monomer that has a wide range of applications in water treatment, medicine, etc. [21,22]. Similarly, 2-acrylamido-2-methyl-1-propane sulfonic acid sodium salt (AMPS) as an anionic monomer has received attention due to its strongly ionizable sulfonate group [23].

Biopolymers functionalized with ionic monomers with DMDMAC and AMPS can be potential adsorbents for removal of ionic dyes from effluents. Methylene blue is one of the most widely used synthetic dyes in fibre industries for dyeing wool and silk. Despite its potential applications in the textile and leather industries,

the MB dye is considered as a potent carcinogen, recalcitrant and toxic to mammalian cells [24].

Zhou et al. [25], synthesised a cellulose-graft-poly(acrylic acid) hydrogels via free radical polymerisation in phosphoric acid solution and evaluated its capacity towards adsorption of MB from aqueous solution. The results showed that the graft polymer possesses an excellent affinity towards MB with maximum adsorption capacity of 2197 mg/g.

Ghorai et al. [26], reported the synthesis of xanthan gum-graft-polyacrylamide-nano silica composite for the adsorption of methylene blue and methyl violet. The results showed a remarkable higher adsorption of 99.4% and 99.1% efficiency for MB and MV respectively.

The use of lignocellulose-g-poly(acrylic acid)/montmorillonite composite gel for the removal of MB from aqueous solution was reported [27]. The results showed that the maximum adsorption capacity for MB on the composite gel is 1994.38 mg/g. The desorption studies revealed that the composite provided the potential for regeneration and reuse after MB dye adsorption, which implied that the composite could be regarded as a potential adsorbent for cationic dye MB removal in a wastewater treatment process.

The adsorption of MB on sodium alginate-graft-polyacrylamide was reported [28]. The adsorption was observed to be pH dependent with maximum adsorption capacity of 69.13 mg/g recorded at pH 10.

Biopolymers functionalised with ionic monomers such as DADMAC and AMPS can be potential adsorbents for ionic dye from aqueous solution. Hence it was planned to develop a copolymer composite gel of DADMAC and AMPS grafted on LBG and its BNT composite for the removal of MB from aqueous solution.

2. MATERIALS AND METHODS

2.1 Materials

Locust bean gum (LBG), Diallyldimethyl ammonium chloride (DADMAC), 2-acrylamido-2-methyl propane sulfonic acid (AMPS) were purchased from Sigma Aldrich Chemical Company, India, Ammonium peroxodisulphate (APS) and N, N-methylene-bisacrylamide (MBA) were obtained from SpectroChem Pvt. Ltd

Mumbai, India. Methylene blue (MB) was obtained from s. d. fine chemicals Ltd. Mumbai, India. Acetone was obtained from Nice Chemicals pvt Ltd., Kerala, India. Methanol was obtained from Himedia Laboratories Pvt, Ltd., Mumbai, India. All the reagents were used as obtained. Throughout the experiments, distilled water was used.

2.2 Methods

2.2.1 Preparation of LBG-g-poly(DADMAC-co-AMPS) gel

The grafting of poly(DADMAC-co-AMPS) on to LBG was carried out as follows; A fixed amount of LBG (0.1g) was dispersed in 20 mL distilled water and stirred overnight followed by addition of APS (0.008) and stirred for an hour. A specified amount of DADMAC (0.15-0.40g) and AMPS (0.1-0.30g) were added to the above solutions followed by MBA (0.005g) and stirred for 8 hours Nie et al. [29]. The solution was then irradiated in a domestic microwave (LG-Grill-Intellowave, India) at 80 watts for 120 seconds with alternate heating and cooling. The solution was then left overnight at ambient temperature to complete grafting and precipitated out using acetone. The precipitate was separated and washed with methanol 2-3 times to remove the unreacted monomers. The grafted gel was dried in a hot air oven overnight at 50°C.

2.2.2 Preparation of LBG-g-poly(DADMAC-co-AMPS) gel/BNT

The LBG-g-poly(DADMAC-co-AMPS)/BNT composite gel was made following the same procedure as in 2.2.1 above but with addition of BNT under continuous stirring after addition of monomers but prior to microwave irradiation.

2.3 Characterisation

LBG, Poly(DADMAC-co-AMPS), LBG-g-poly(DADMAC-co-AMPS) and LBG-g-poly(DADMAC-co-AMPS)/BNT were characterised using standard techniques. The FTIR spectra were recorded in the wave number range of 4000 to 400 cm⁻¹ during 40 scans, with a resolution of 2 cm⁻¹ using FTIR (Prestige-21, Shimadzu, Japan). The FESEM images were recorded after gold sputtering of the samples in order to make them electrically conductive and scanned at 20 KVA using and JEOL JSM-6380LA (USA) scanning electron microscope. The EDS analysis was carried out using the same FESEM. X-ray diffractograms of the

samples were recorded on a benchtop X-ray diffractometer, Shimadzu XRD-6000 instrument (Japan). The diffraction patterns were recorded over a 2θ range of 0–80° with a resolution of 0.02° Cu K α radiation ($\lambda = 1.5406 \text{ \AA}$, 30 kV, 30 mA) at room temperature at an analysis rate of 2°/min.

2.4 Dye Adsorption Study

The adsorption study was carried out in a solution of 100 mg/L of MB solution with a known amount of LBG-g-poly(DADMAC-co-AMPS) and LBG-g-poly(DADMAC-co-AMPS)/BNT. The gel and composite samples were immersed in the dye solution and at different time interval 1mL of the solution was withdrawn and diluted appropriately, and the absorbance was measured using UV-visible spectrophotometer (UV-1800 SHIMADZU, Japan) at λ_{max} of 610 nm. Predetermined calibration curves were used to convert the absorbance values into concentration. Equilibrium adsorption studies were also carried out using different dye concentrations (10–100 mg/L). The amount of dye adsorbed at time t and at equilibrium was calculated from the following equations [30].

$$q_t = \frac{(C_o - C_t) \times V}{M}$$

$$q_e = \frac{(C_o - C_e) \times V}{M}$$

Where q_t and q_e are the amount of MB adsorbed (mg/g) at time $t = t$ and at equilibrium respectively. C_o , C_t and C_e are dye concentrations (mg/L) at time $t = 0$, $t = t$ and at equilibrium respectively. M is the weight of the samples (g) and v is the volume (L) of the MB solution used for adsorption.

3. RESULTS AND DISCUSSION

3.1 Preparation of LBG-g-poly(DADMAC-co-AMPS)

The initiator APS under microwave heating generates sulphate anion radicals that attack the LBG and abstract the hydrogen radicals thereby creating reactive sites on LBG molecules (macroradicals). During the polymerisation process, grafting of the copolymer consisting of repeating units of AMPS and DADMAC occurs on LBG macroradicals. The presence of the bi-functional MBA in the copolymer chain results in the formation of a gel network of LBG-g-

poly(DADMAC-co-AMPS). The presence of inorganic BNT during the polymerisation process which acts as fillers leads to the formation of clay entrapped LBG-g-poly(DADMAC-co-AMPS)/BNT gel composite. The general reaction mechanism for the formation of LBG-g-poly(DADMAC-co-AMPS) in the presence of APS and MBA is shown in Scheme 1.

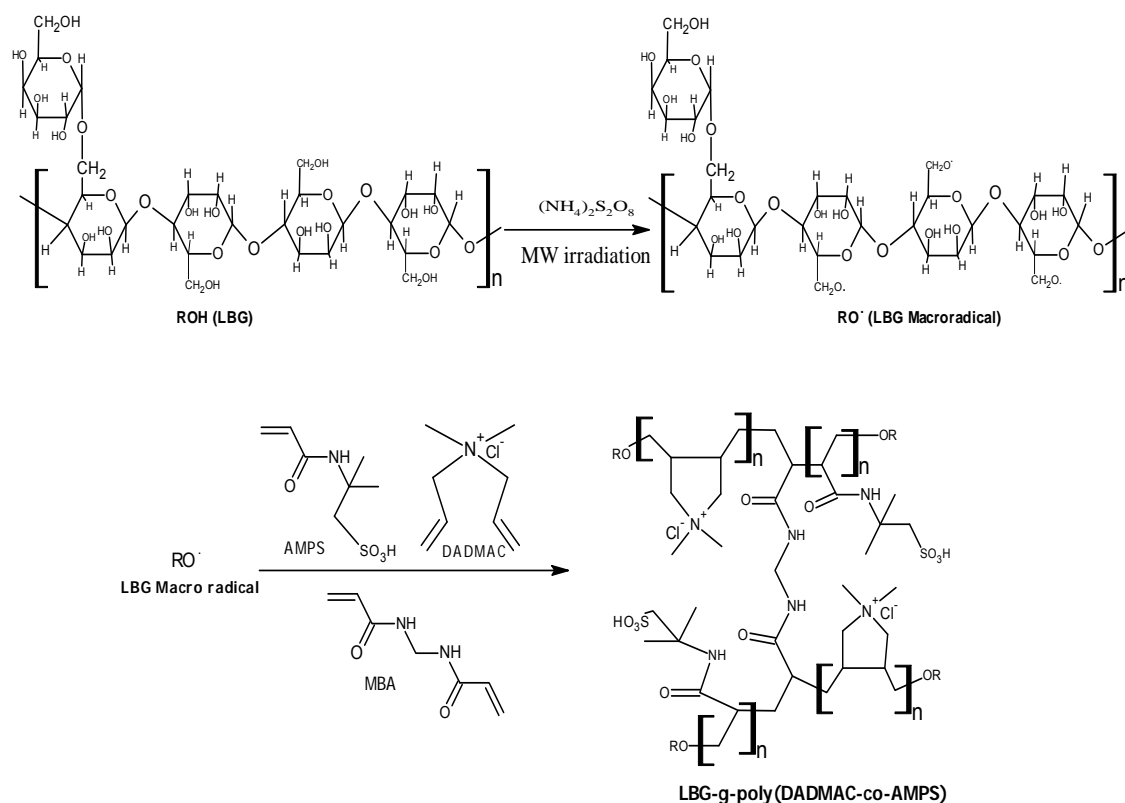
3.2 Characterization

3.2.1 FTIR spectroscopy

The FTIR spectra of LBG, poly(DADMAC-co-AMPS), LBG-g-poly(DADMAC-co-AMPS) and LBG-g-poly(DADMAC-co-AMPS)/BNT are presented in Fig. 1. The LBG spectrum (Fig. 1a) showed a broadband at 3350 cm^{-1} which are attributed to O-H stretching. The band at 2910 cm^{-1} is assigned to C-H₂ bending/wagging vibration [31]. The band observed at 1010 cm^{-1} is due to C-O-H stretching. The spectrum of poly(DADMAC-co-AMPS) (Fig. 1b) shows an -N-H stretching band at 3426 cm^{-1} , C-H stretching at 2913 cm^{-1} , C-N stretching around 1474 cm^{-1} , C=O stretching of amide at 1615 cm^{-1} , a weak band at 650 cm^{-1} due to S-O stretching vibration. For LBG-g-poly(DADMAC-co-AMPS) (Fig. 1c), in addition to the bands observed in Fig. 3.1a, bands at 1535 cm^{-1} and 1720 were observed due to N-H bending and C=O stretching respectively. In the spectrum of LBG-g-poly(DADMAC-co-AMPS)/BNT shown in Fig. 1d, there is a shift in C=O stretching vibration from 1720 to 1649 cm^{-1} and additional occurrence of new bands at 1017, 939 and 808 cm^{-1} for Si-O-Si stretching, Si-O-Al bending and Si-O-C stretching respectively which provides evidence for incorporating BNT into the system.

3.2.2 FESEM analysis

The surface morphology of LBG, poly(DADMAC-co-AMPS), LBG-g-poly(DADMAC-co-AMPS) and LBG-g-poly(DADMAC-co-AMPS)/BNT samples are presented in Fig. 2. The smooth, porous and inhomogeneous surface structure of LBG (Fig. 2a) undergoes significant change on gel formation. The poly(DADMAC-co-AMPS) shows a smooth surface (Fig. 2b) compared to LBG. The LBG-g-poly(DADMAC-co-AMPS) (Fig. 2c) surface appears cotton-like and irregular. The incorporation of BNT into the system (Fig. 2d) produces a coarse and undulant surface with higher porosity compared to LBG-g-poly(DADMAC-co-AMPS).



Scheme 1. Proposed scheme for the formation of LBG-g-poly(DADMAC-co-AMPS)

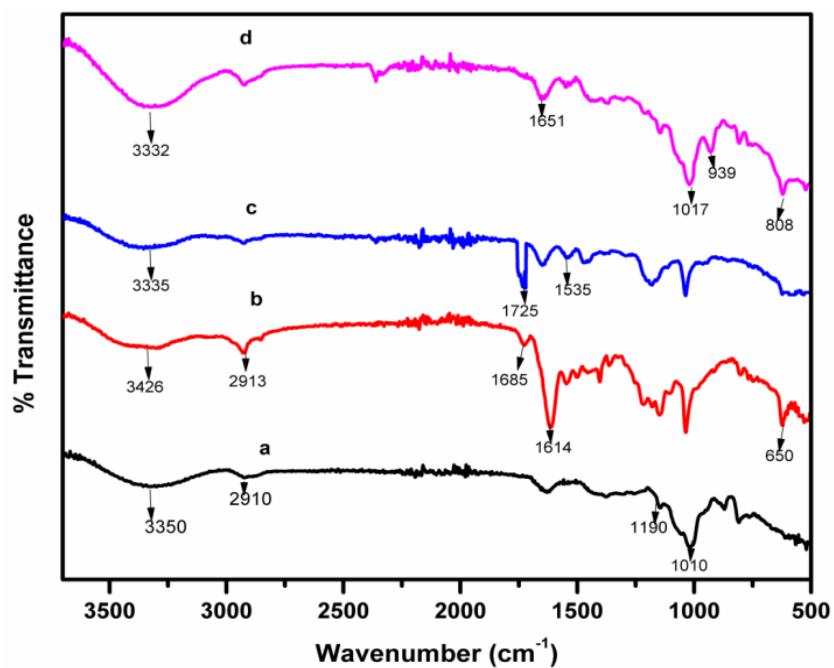


Fig. 1. FTIR spectra of: a) LBG, b) poly(DADMAC-co-AMPS), c) LBG-g-poly(DADMAC-co-AMPS) and d) LBG-g-poly(DADMAC-co-AMPS)/BNT

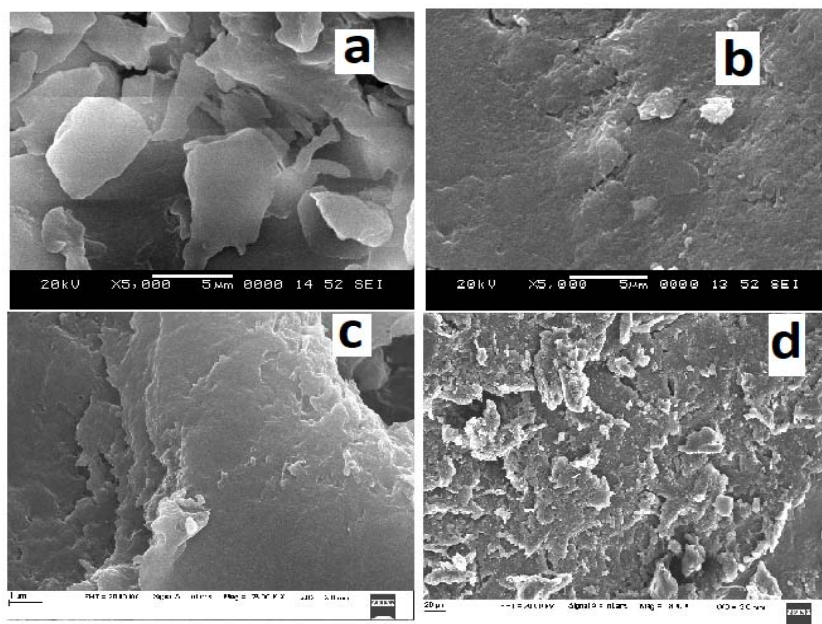


Fig. 2. FESEM images of; a) LBG, b) Poly(DADMAC-co-AMPS), c) LBG-g-poly(DADMAC-co-AMPS) and d) LBG-g-poly(DADMAC-co-AMPS)/BNT

3.2.3 EDS

The composition of LBG-g-poly(DADMAC-co-AMPS)/BNT was investigated using EDS and the EDS spectrogram (Fig. 3) shows elemental

distribution over the surface of LBG-g-poly(DADMAC-co-AMPS)/BNT. The presence of Al, Si, Fe and Na peaks in addition to C, N, O and Cl confirmed the incorporation of BNT within the graft copolymer.

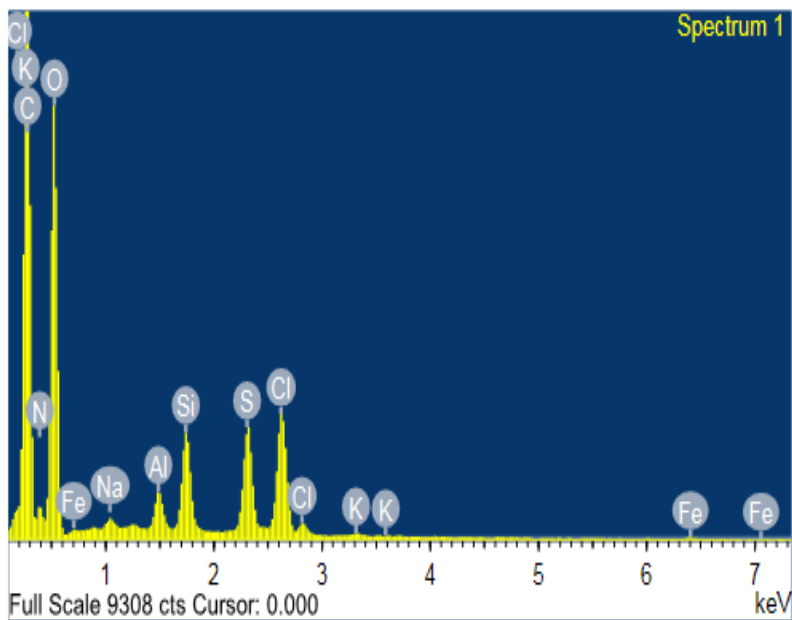


Fig. 3. EDS image of LBG-g-poly(DADMAC-co-AMPS)/BNT

3.2.4 XRD

The XRD patterns of LBG, BNT, LBG-g-poly(DADMAC-co-AMPS) and LBG-g-poly(DADMAC-co-AMPS)/BNT are shown in Fig. 4. The LBG shows no considerable peak of crystallinity (Fig. 4a), hence proved its amorphous nature as reported by [32]. The diffractogram of BNT (Fig. 4b) shows the crystalline peaks at 2θ values of 19.76° , 26.5° , 34° and 62° . Fig. 4c shows clearly that LBG-g-poly(DADMAC-co-AMPS) is amorphous as no crystalline peak is observed in diffractogram. The degree of incorporation of BNT within the graft copolymer (Fig. 4d) shows clearly that the highest crystalline peaks ($2\theta=26.5^\circ$ and 62°) that are present in the pure LBG has diminished in the LBG-g-poly(DADMAC-co-AMPS)/BNT. This clearly showed that BNT has been incorporated within the graft-copolymer network.

3.3 Adsorption of MB

The adsorption studies was carried out using MB as model dye.

➤ Effect of contact time

The effect of contact time on the adsorption capacity of LBG-g-poly(DADMAC-co-AMPS) and LBG-g-poly(DADMAC-co-AMPS)/BNT towards MB is shown in Fig. 5. Initially, the adsorption on both adsorbents proceeded slowly up to 30 minutes and gradually 420 minutes for the LBG-g-poly(DADMAC-co-AMPS)/BNT and 180 minutes for LBG-g-poly(DADMAC-co-AMPS). Fast adsorption was observed between 420 to 540 minutes on all the adsorbents. The adsorption of equilibrium was reached between 540 to 600 minutes. The equilibrium adsorption capacity for MB was found to 65.09 and 70.89 mg/g respectively for LBG-g-poly(DADMAC-co-AMPS) and LBG-g-poly(DADMAC-co-AMPS)/BNT. The adsorption of MB is attributed to the electrostatic interaction between the adsorbents and the asorbates. The higher adsorption by LBG-g-poly(DADMAC-co-AMPS)/BNT compared to LBG-g-poly(DADMAC-co-AMPS) is attributed to H-bonding interactions as well as dipole-dipole and electrostatic interactions between anionic site of BNT and cationic site of MB molecules [26].

3.3.1 Adsorption kinetics

The kinetics study for the adsorption of MB was investigated using the two most commonly used kinetic models. The are;

➤ Lagergren Pseudo First Order Kinetics

The pseudo first order kinetic model is expressed by the linear relationship [33] by the following equation.

$$\log(q_e - q_t) = \log q_e - \frac{K_1}{2.303} t$$

Where q_e and q_t are the amount of MB (mg/g) adsorbed at equilibrium and at time t respectively, k_1 is the rate constant (min^{-1}) for the pseudo-first order kinetics and t is the time (min.). The rate constant (k_1) and correlation coefficient were calculate from the plot of $\log(q_e - q_t)$ vs t (Fig. 6) and tabulated in Table 1. It was observed from the data presented in Table 1 that there is no agreement between the $q_{e(\text{cal})}$ and $q_{e(\text{exp})}$. Also, the R^2 values are low in all cases, hence adsorption of MB onto LBG-g-poly(DADMAC-co-AMPS) and LBG-g-poly(DADMAC-co-AMPS)/BNT cannot be well explained by the pseudo-first-order kinetic model.

➤ Pseudo Second Order Kinetics

The linear form of the pseudo second order kinetic equation [34] is represented by the following equation;

$$\frac{t}{q_t} = \frac{1}{k_2 q_e^2} + \frac{1}{q_e} t$$

Where q_e and q_t are as defined earlier, k_2 is the second order rate constant (g/mg/min). The plot of t/q_t vs t (Fig. 7) gives a straight line from which it can be concluded that the adsorption of MB is well explained by pseudo second order kinetic process. This indicated that adsorption's mechanism is chemically rate controlling (chemisorptions). The values of q_e , k_2 and R^2 obtained from the intercept and slope of t/q_t vs t plots (Fig. 7) are presented in Table 1. The R^2 values are 0.957 and 0.953 respectively on LBG-g-poly(DADMAC-co-AMPS) and LBG-g-poly(DADMAC-co-AMPS)/BNT. Furthermore, the values of $q_{e(\text{cal})}$ obtained from pseudo second order are in good agreement with the $q_{e(\text{exp})}$ compared to pseudo first order kinetic model.

3.3.2 Adsorption isotherms

For equilibrium adsorption studies, fixed amount (0.05g) of the adsorbents were used in 25mL solution containing a varied concentration of MB (10-100 mg/L) and the maximum amount of MB adsorbed in each case was determined. The two isotherm models namely; Freundlich [35] and Langmuir [36] were employed in this work to

understand the adsorption behaviour of the dyes on the adsorbents.

➤ Freundlich Isotherm

The Freundlich isotherm model assumes multilayer adsorption. It is based on the assumption that encompasses the heterogeneity of the surface and the adsorption capacity is related to the equilibrium concentration of the adsorbate. The Freundlich isotherm is commonly expressed as;

$$\ln q_e = \ln k_f + \frac{1}{n} \ln C_e$$

Where q_e and C_e are the amount of MB adsorbed (mg/g) and the equilibrium concentration of MB (mg/L) respectively, k_f (mg/g) and n are Freundlich adsorption isotherm constants that represent the adsorption capacity of MB and the degree of nonlinearity between the MB concentration and the adsorbents respectively. The values of k_f and n were calculated from the intercept and slope of the plot of $\log q_e$ vs $\log C_e$ (Fig. 8) and are presented in Table 2. The adsorption of MB on LBG-g-poly(DADMAC-co-AMPS) and LBG-g-poly(DADMAC-co-AMPS)/BNT is considered to be favourable ($n=1-10$). Similarly, the value of R^2 in all cases are higher and move towards unity which is an indication of the fitting of adsorption data into the model.

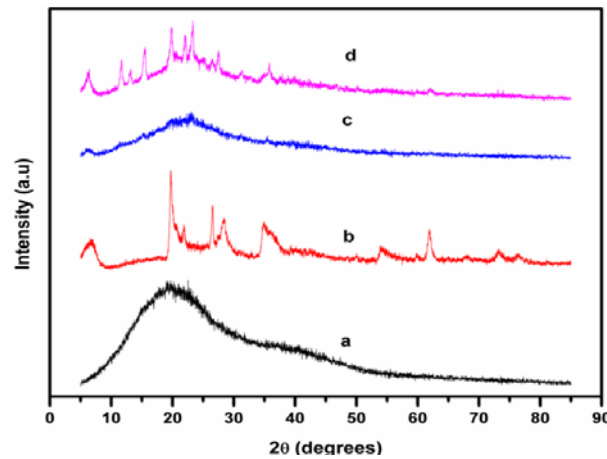


Fig. 4. XRD images of; a) LBG, b) BNT, c) LBG-g-poly(DADMAC-co-AMPS) and d) LBG-g-poly(DADMAC-co-AMPS)/BNT

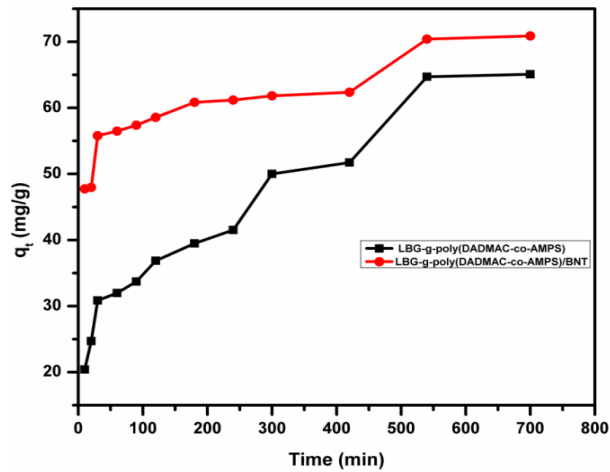


Fig. 5. Effect of contact time on the adsorption of MB on the adsorbents (adsorbent dose=120 mg; $C_0 = 100$ mg/L; $V=100$ mL and pH 7.0)

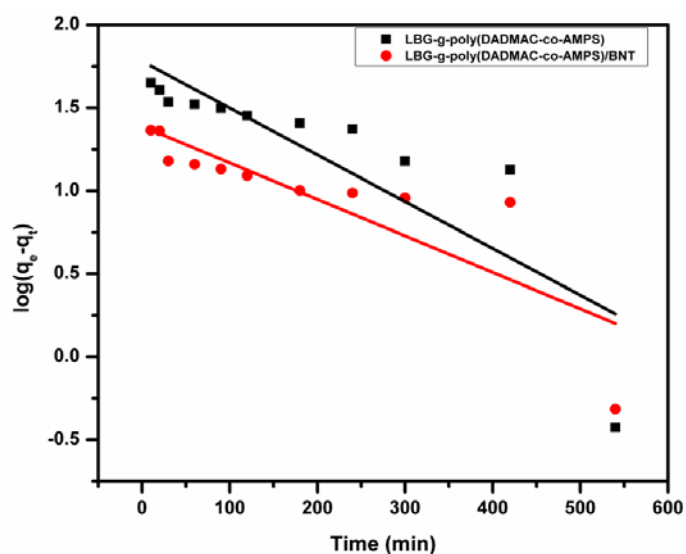


Fig. 6. Pseudo first order kinetic for the adsorption of MB the adsorbents

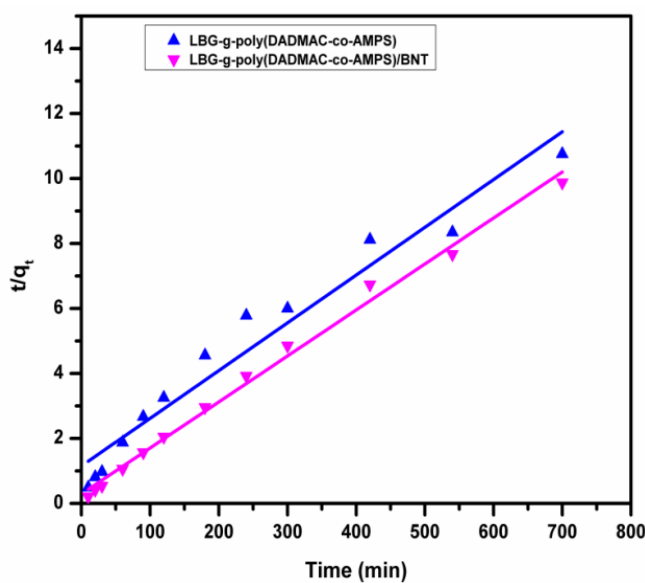


Fig. 7. Pseudo second order kinetic for the adsorption of MB onto adsorbents

Table 1. Kinetics data for the adsorption of MB

Parameters	LBG-g-poly(DADMAC-co-AMPS)	LBG-g-poly(DADMAC-co-AMPS)/BNT
$q_e \text{ exp. (mg/g)}$	65.09	70.89
$q_{ecal} \text{ (mg/g)}$	60.26	24.43
First $k_1 \text{ (min}^{-1}\text{)}$	0.006	0.005
R^2	0.719	0.717
$q_{ecal} \text{ (mg/g)}$	71.43	71.43
Second $k_2 \text{ (g/g/min)}$	0.002	0.0007
R^2	0.957	0.993

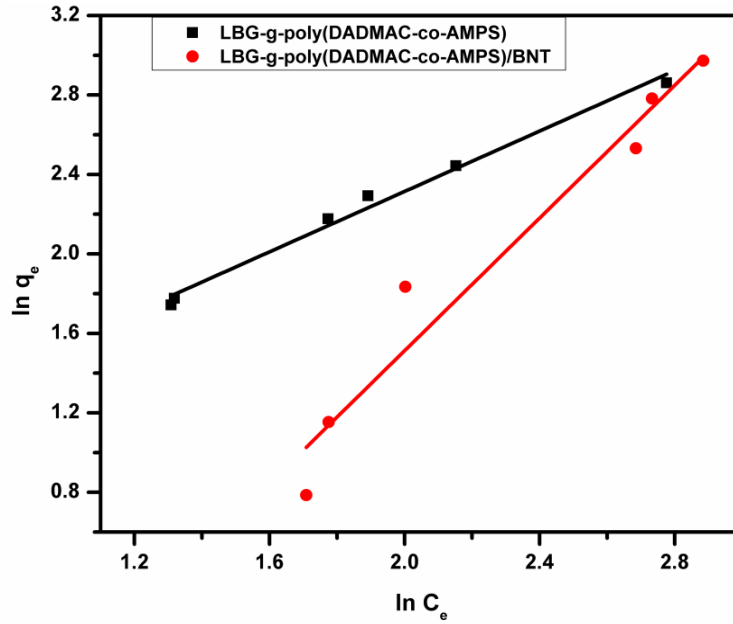


Fig. 8. Freundlich isotherm for MB onto the adsorbents

The value of k_f obtained from both adsorbents are low compared to 2.51 mg/g obtained by Pathania et al. [5] for activated carbon, 75.2 mg/g by El Moouzdahir et al. [37] on Moroccan clay and 13.6 mg/g by Yao et al. [38] on carbon nanotubes.

➤ Langmuir Model

The Langmuir isotherm is a model which quantitatively describes the formation of the equilibrium monolayer of adsorbate molecules on the surface of the adsorbent and is expressed as follows;

$$\frac{C_e}{q_e} = \frac{1}{q_m} \cdot C_e + \frac{1}{K_L q_m}$$

Where C_e and q_e are as defined earlier, q_m is the maximum adsorption corresponding to complete monolayer coverage on the surface (mg/g) and K_L is the Langmuir constant which is related to the energy of adsorption (L/mg). K_L and q_m are determined from the intercept and slope of the linear plot of C_e/q_e vs C_e (Fig. 9). The essential feature of the Langmuir isotherm can be represented in terms of separation factor (dimensionless equilibrium parameter) R_L [39], which can be expressed as;

$$R_L = \frac{1}{1 + K_L C_0}$$

where, C_0 is the initial concentrations of MB, K_L is the constant related to the energy of adsorption (Langmuir Constant). R_L value indicates the favorability of adsorption. If $R_L > 1$ the adsorption is unfavorable, if $R_L = 1$ the adsorption is linear, if $0 < R_L < 1$ the adsorption is favourable and if $R_L = 0$ then the adsorption is irreversible.

The Langmuir isotherm data are presented in Table 2. The R_L values obtained in this study showed favourable adsorption of MB on the gel.

The maximum adsorption capacity (q_m) of 43.38 and 10.75 mg/g on the gel and composite respectively are low compared to values obtained by Pathania et al. [5] (47.62 mg/g) for activated carbon, Elmoouzdahir et al. [37] (142 mg/g) on Moroccan clay and Yao et al. [38] (35.4 mg/g) on carbon nanotubes.

3.3.3 Desorption studies

One of the most important features of the adsorbent is its regeneration ability. This is because it simplifies the sewage treatment manipulation, save cost and increase the disposal efficiency of dye wastewater [40]. Fig. 10 showed the percentage desorption of MB in the acidic and alkaline medium. It was observed that a higher amount of MB on the composites was recovered in both acidic and alkaline medium.

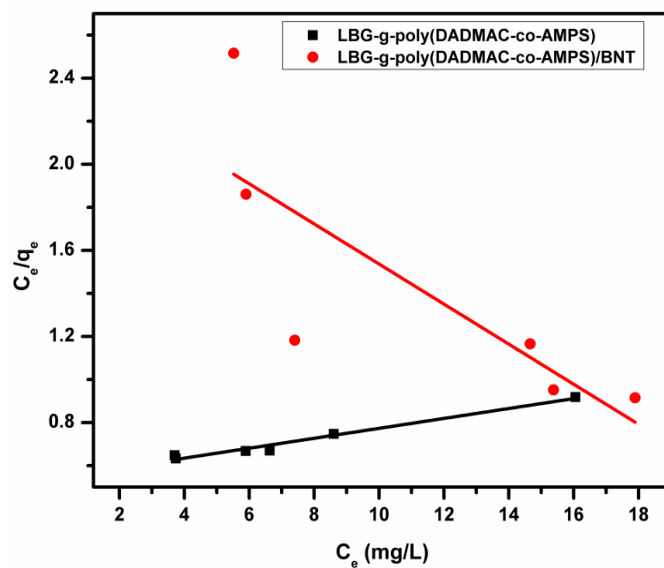


Fig. 9. Langmuir isotherm for MB onto the adsorbents

Table 2. Adsorption isotherms data for MB

Parameters		LBG-g-poly(DADMAC-co-AMPS)	LBG-g-poly(DADMAC-co-AMPS)/BNT
Freundlich	n	1.32	0.60
	k_f (mg/g)	2.21	0.16
	R^2	0.989	0.956
Langmuir	q_{max} (mg/g)	43.48	10.75
	R_L	0.70	1.60
	k_L (L/mg)	0.042	0.04
	R^2	0.978	0.648

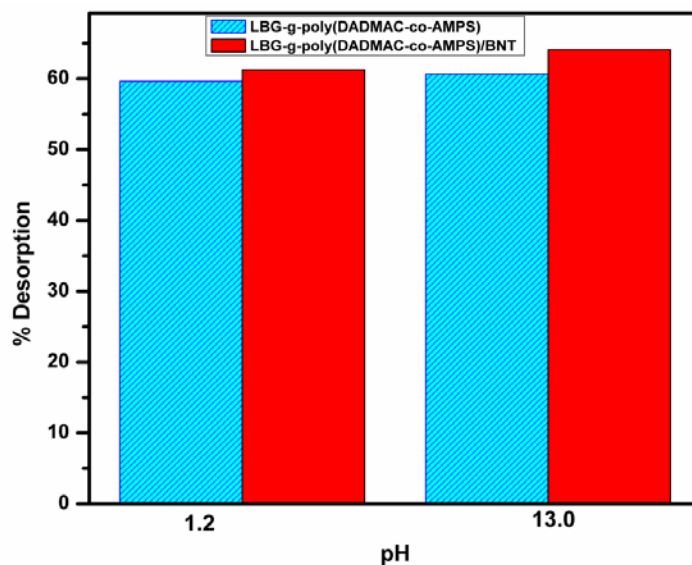


Fig. 10. % desorption of the adsorbed MB from the adsorbents

4. CONCLUSION

In the present study, a graft-copolymer gel consisting of LBG, DADMAC, AMPS and its composite with BNT clay were made via microwave irradiation. The adsorption of MB on the graft-copolymer gel and the composite revealed that MB was adsorbed more on both LBG-g-poly(DADMAC-co-AMPS)/ BNT than LBG-g-poly(DADMAC-co-AMPS). The adsorption data were observed to fit best into the Freundlich model and the adsorption is found to follow second-order kinetic model.

COMPETING INTERESTS

Authors have declared that no competing interests exist.

REFERENCES

1. Malana, M. A., Ijaz, S. and Ashiqm, M. N. (2010). *Desalination*, **263**: 249-257.
2. Zhou, C., Wu, Q., Lei, T and Negulescu, I. I. (2014). *Chem. Eng. J.*, **251**: 17-24.
3. Gan, L., Shang, S., Hu, E., Yuen, C. W. M. and Jiang, S. (2015). *Appl. Sur. Sci.*, **357**: 866-872.
4. Fosso-kankeu, E., Mittal, H., Mishra, S. B. and Mishra, A. K. (2015). *J. Ind. Eng. Chem.*, **22**: 171-178.
5. Pathania, D., Sharma, S. and Singh, P. (2017). *Arab. J. Chem.*, 10(1): S1445-S1451
6. Santos, S. C. R., Boaventura, R. A. R. (2016). *J. Environ. Chem. Eng.*, **4**: 1473–1483.
7. Mahida, V. P., Patel, M. P. (2016). *Chin. Chem. Lett.*, **27**: 471–474.
8. Maity, J., Ray, S. K. (2016). *Int. J. Biol. Macromol.*, **89**: 246-255.
9. Robati, D., Mirza, B., Ghazisaeidi, R., Rajabi, M., Moradi, O., Tyagi, I., Agarwal, S., Gupta, V. K. (2016). *J. Mol. Liq.*, **216**: 830–835.
10. Kaity, S., Isaac, J., Kumar, P. M., Bose, A., Wong, T. W. and Ghosh, A. (2013). *Carbohydr. Polym.*, **98**: 1083–1094
11. Kaity, S. and Ghosh, A. (2013). *Ind. Eng. Chem. Res.*, **52**: 10033–10045
12. Nisperos-Carriedo, M. O. (1994). Edible coatings and films based on polysaccharides. In: Krochta, J. M., Baldwin, E. A., Nisperos-Carriedo, M.O., (eds), *Edible films and coatings to improve food quality*. Lancaster: Technomic, 305–36.
13. Maiti, S., Dey, P., Banik, A., Sa, B., Ray, S. and Kaity, S. (2010). *Drug Del.*, **17**(5): 288–300
14. Sundaram, J. and Durance, T. D. (2008). *Food Hydrocolloids*, **22**: 1352–1361
15. Kawamura, Y. (2008). Carob bean gum chemical and technical assessment (CTA) for the 69th JECFA. Page 1-6
16. Sebastian, S., Mayadevi, S., Beevi, B. S., Mandal, S. (2014). *J. Water Res. Prot.*, **6**: 177-184.
17. Gupta, S. K., Nayunigari, M. K., Misra, R., Ansari, F. A., Dionysiou, D. D., Maity, A., Bux, F. (2016). *Ind. Eng. Chem. Res.*, **55**: 3–20.
18. El Haddad, M., Mamouni, R., Saffaj, N., Lazar, S. (2012). *Glob. J. Hum. Soc. Sci. Geog. & Environ. Geo-Sci.*, **12**: 19-29
19. Patil, M. R., Shrivastava, V. S. (2015). *J. Mater. Environ. Sci.*, **6**: 11-21
20. Tirelli, N. and Hunkeler, D. J. (1999). *Macromol. Chem. Phys.*, **200** (5): 1068-1073
21. Jing, R. and Hongfei, H. (2001). *Eur. Polym. J.*, **37**: 2413-2417.
22. Zhao, Q., Sun, J., Chen, S and Zhou, Q. (2010). *J. Appl. Polym. Sci.*, **115**(5): 2940-2945.
23. Durmaz, S. and Okay, O. (2000). *Polymers*, **41**(10): 3693–3704.
24. Gopi, S., Balakrishnan, P., Piusa, A. and Thomas, S. (2017). *Carbohydr. Polym.*, **165**: 115–122.
25. Zhou, Y., Fu, S., Liu, H., Yang, S. and Zhan, H. (2011). *Polym. Eng. Sci.*, **51**: 2417-2422
26. Ghorai, S., Sarkar, A., Raoufi, M., Panda, A. B., Schö nherr, H. and Pal, S. (2014). *ACS App. Mat. Interfaces*, **6**: 4766–4777
27. Shi, Y., Xue, Z., Wang, X., Wang, L. and Wang, A. (2013). *Polym. Bull.*, **70**: 1163–1179
28. da Feira, J. M. C., Klein, J. M. and Forte, M. M. D. C. (2018). *Polímeros*, **28**(2): 139-146
29. Nie, X., Adalati, A., Du, J., Liu, H., Xu, S. and Wang J (2014). *Appl. Clay Sci.*, **97**–**98**: 132–137
30. Karthika, J. S. and Vishalakshi, B. (2015). *Int. J. Biol. Macromol.*, **81**: 544–655
31. Kaity, S., Isaac, J., Ghosh, A. (2013). *Carbohydr. Polym.*, **94**: 456–467

32. Martins, J. T., Cerguira, M. A., Bourbon, A. I., Pinheiro, A. C., Souza, B. W. S., Vicente, A. A. (2012). *Food Hydrocolloids*, **29(2)**: 280-289
33. Lagergren, S. (1898). K. Sven. Vetenskapsakad. Handl.,. **24 (4)**: 1-39.
34. Ho, Y. S. and McKay, G. (1998). *Trans Ichem E*, **76 Part B**: 332- 340
35. Freundlich, H., Heller, W. (1939). *J. Am. Chem. Soc.*, **61(8)**: 228-230
36. Langmuir, I. (1916). *J. Am. Chem. Soc.*, **38 (11)**: 2221–2295
37. El Mouzdahir, Y., Elmchaouri, A., Mahboub, R., Gil, A. and Korili, S. A. (2007). *J. Chem. Eng. Data*, **52**: 1621-1625
38. Yao, Y., Xu, F., Chen, M., Xu, Z. and Zhu, Z. (2010). *Bioresour. Technol.*, **101(9)**: 3040-3046
39. Krishna, R. H., & Swamy, A. V. (2012). *Int. J. Eng. Res.Dev.*, **4 (1)**: 29-38.
40. Chen, M., Ding, W., Wang, J., Diao, G. (2013). *Ind. Eng. Chem. Res.*, **52(6)**: 2403–2411